Effects of Disulfide Bridges in Domain I of *Bacillus thuringiensis* Cry1Aa δ-Endotoxin on Ion-Channel Formation in Biological Membranes

O. Alzate,*[,‡,§,||] T. You,[‡,⊥] M. Claybon,[‡] C. Osorio,[‡] A. Curtiss,[‡] and D. H. Dean[‡]

Biochemistry Department, The Ohio State University, 484 West 12th Avenue, Columbus, Ohio 43210, and Parque Tecnológico de Antioquia, Medellín, Colombia

Received July 20, 2006; Revised Manuscript Received September 13, 2006

ABSTRACT: The δ-endotoxin family of toxic proteins represents the major component of the insecticidal capability of the bacterium *Bacillus thuringiensis*. Domain I of the toxins, which is largely α-helical, has been proposed to unfold at protein entry into the membrane of a target insect, following models known as the penknife and umbrella models. We extended the analysis of a previous work in which four disulfide bridges were constructed in domain I of the Cry1Aa δ-endotoxin that putatively prevented unfolding during membrane partitioning. Using bioassays and voltage clamping of whole insect midgut instead of artificial lipid bilayers, it was found that, while toxicity and inhibition of the short-circuit current were reduced, only one of the disulfide bridges eliminated the activity of the toxins in the insect midgut membrane, and in that case, the loss of toxicity was due to the single amino acid substitution, R99C. It is proposed that at least α helices 4, 5, 6, and 7 and domain II partition in the midgut membranes of target insects, in support of an insertion model in which the whole protein translocates into the midgut membrane.

The partition of water-soluble proteins into biological membranes is an important step in the mode of action of some bacterial pathogens. One of these pathogens, *Bacillus thuringiensis* (*Bt*),[1] produces protein toxins with insecticidal capabilities that intoxicate by penetrating the midgut membrane of susceptible insects, thus inducing ion pores that disrupt the membrane potential. The Cry1A family of *Bt* toxins (also known as Cry1A δ-endotoxins) are released as 135 kDa protein molecules that become activated in the insect midgut by the proteolytic action of trypsin-like proteases. The 65 kDa activated toxins bind to specific receptors on the insect midgut lining columnar cells and possibly undergo conformational changes followed by membrane permeation and ion-channel formation, eventually resulting in the death of the insect (*1*).

The activated Cry1Aa toxin (*2*) [Protein Data Bank (PDB) code 1CIY] is a cysteine-free protein composed of three distinct structural domains (Figure 1). Domain I contains seven α helices that account for 85−90% of the secondary structure of this domain. These α helices are numbered 1−7, with the highly hydrophobic α helix 5 located in the center and the other six surrounding it (Figure 1). As result of

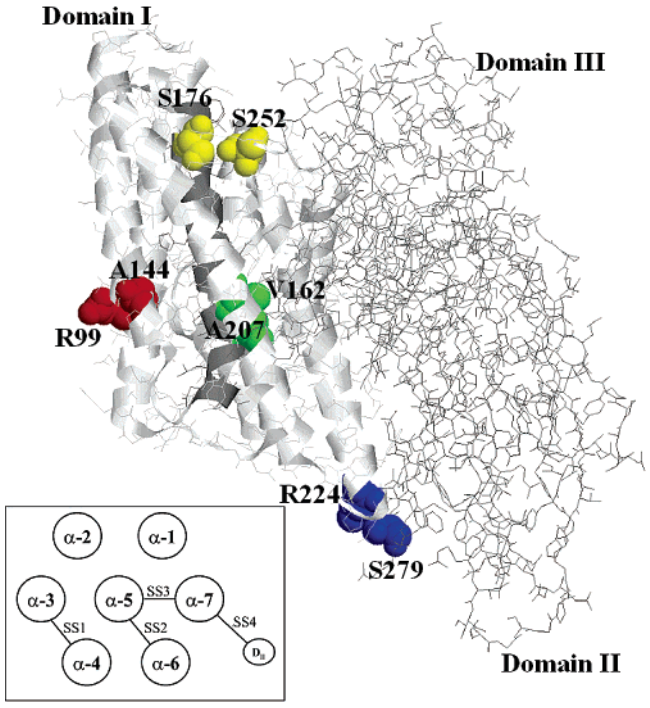

FIGURE 1: Three-dimensional structure of Cry1Aa displaying three structural domains. Domain I is shown on the left in a ribbon-like representation. The highly hydrophobic α helix 5 is shown in dark gray. Disulfide bridge SS1 (C99−C144) producing a link between α helices 3 and 4 is shown in red. SS2, in green, is designed such that the external α helix 6 is locked to the inner α helix 5 (162C−207C). SS3, in yellow, holds together α helices 5 and 7 through a linkage between C176 and C252. SS4, the only non-interhelical link, forms a bridge between α helix 7 (C224) and domain II (C279), shown in blue. Domains II and III are shown in a wire-frame representation on the right. The inset shows a diagram highlighting the disulfide linkages.

* To whom correspondence should be addressed: Neuroproteomics Center, Department of Neurobiology, Duke University Medical Center, 258 Bryan Research Building, DUMC Box 3209, Durham, NC 27710. Telephone: (919) 681-5855. Fax: (919) 668-0631. E-mail: alzate@neuro.duke.edu.

‡ The Ohio State University.

§ Parque Tecnológico de Antioquia.

|| Current address: Neuroproteomics Center, Department of Neurobiology, Duke University Medical Center, DUMC Box 3209, Durham, NC 27710.

⊥ Current address: Department of Biological Sciences, Campbell University, Buies Creek, NC 27506.

[1] Abbreviations: BBMV, brush border membrane vesicles; *Bt*, *Bacillus thuringiensis*; β-ME, β-mercaptoethanol; CD, circular dichroism.

10.1021/bi061474z CCC: $33.50
Published on Web 10/21/2006

extensive research for the past 10 years, it has been found that the major functions of domain I are insertion into the midgut membrane and ion-channel formation (*2*−*4*) and that the major functions of domains II and III are involved in receptor binding (*5*−*9*).

The mechanism of δ-endotoxin partitioning into cell membranes has been proposed as resulting from conformational changes induced by the binding process, either the presence of the receptor, the cell membrane, or both; a process not yet elucidated. Two main ideas have been used to model the membrane-bound state of the δ-endotoxins in the target membrane. These theories are known as the "penknife" model (*10*) and the "umbrella" model (*3*). The "penknife" model proposes that α helices 5 and 6 flip out of the domain and insert into the plasma membrane as a helical hairpin. This model is derived from the distribution of the hydrophobic faces of the helices and does not require subsequent rearrangement of the other helices of domain I. The second idea, the "umbrella" model, proposes that α helices 4 and 5 insert into the membrane as a helical hairpin and the other helices flatten out on the membrane surface with their hydrophobic faces facing the membrane. Both models propose that domain II binds to the receptors and triggers conformational changes needed for protein translocation. Both theories were proposed mainly on the basis of analogous properties with other membrane-translocating proteins of similar structure. One such protein, colicin A, was used in support for both the "penknife" (*11*) and "umbrella" (*12*) models.

Two studies using artificial phospholipid vesicles concluded that α helices 4 and 5 are important in driving insertion, thus giving support to the "umbrella" model. The first of these discusses the introduction of disulfide bonds into Cry1Aa to immobilize various α helices of domain I (*4*). The double-cysteine mutants under study were each expected to form one disulfide bridge with the following α helices bound: 3−4, 5−6, 5−7, and 7−loop in domain II. These mutations produced trypsin-resistant activated toxins, whose formation of ion channels in artificial phospholipid vesicles was prevented. After the addition of β-mercaptoethanol (β-ME), ion transport was recovered. The results of this work are very interesting for *Bt* studies on artificial phospholipid vesicles. It follows from this work that studies on real insect midgut membranes under physiological conditions, including bioassays and ion-channel formation, might be useful to gain a better understanding of the mode of action of these important biopesticides. The second study used artificial peptides emulating the α helices of domain I (*13*). This study explored the ability of these individual α-helical peptides to insert into artificial phospholipid vesicles by themselves. The results support the insertion of α helices 4 and 5 into the artificial membrane. Again, these results are attractive and invite us to perform protein translocation studies under physiological conditions on insect midguts.

In addition to the umbrella and penknife models, an alternative model has gained support in recent years. This model proposes that other regions of the protein and probably the whole toxin insert into the target membrane. Adding to previous studies on the insertion of α helices 4 and 5, it was established conclusively that α helix 7 is buried in the membrane and is involved in ion transport (*14*, *15*). One review introduced a revised model, stating that domain III, as well as domain I, inserts into the target membrane (*16*). Other studies suggest that the whole toxin inserts into the cell membrane (*17*−*20*). This new hypothesis supports a mechanism for protein−membrane interaction in which the entire protein, with the possible exception of α helix 1, inserts into the membrane. This mechanism probably involves multimeric protein conformations (*18*, *21*). Even with the extensive research that has been performed to uncover the insertion mechanism of Cry1Aa, current models do not account for all of the experimental observations.

Table 1: Double-Cysteine Mutations Introduced in the Cry1Aa δ-Endotoxin[a]

mutant protein	original residues	expected α-helices bound	bond length, C_α (Å)	bond length, C_β (Å)
SS1	Arg99−Ala144	3−4	5.777	4.057
SS2	Val162−Ala207	5−6	7.056	5.466
SS3	Ser176−Ser252	5−7	6.999	4.594
SS4	Arg224−Ser279	7−domain II	5.033	3.549

[a] The bond lengths given were determined with RasMol from the crystal structure of the wild-type toxin (PDB code 1CIY).

For the present study, eight cysteine mutations identical to those mutants produced previously by Schwartz et al. (*4*) were constructed (see Table 1 and Figure 1). In total, six different Cry1Aa mutant proteins were developed, four containing a different double-cysteine mutation expected to form a disulfide bridge and two single-mutant proteins. The disulfide bridge mutant proteins were named SS1, SS2, SS3, and SS4. SS1 (Arg99Cys−Ala144Cys) is expected to form a disulfide bridge between α helices 3 and 4; SS2 (Val162Cys−Ala207Cys) is expected to form a disulfide bridge between α helices 5 and 6; SS3 (Ser176Cys−Ser252Cys) is expected to form a disulfide bridge between α helices 5 and 7; and SS4 (Arg224Cys−Ser279Cys) is expected to form a disulfide bridge between α helix 7 and a loop at the beginning of domain II, respectively (Figure 1 and Table 1).

MATERIALS AND METHODS

Site-Directed Mutagenesis. Amino acid residues for site-directed mutagenesis were selected as published by Schwartz et al. (*4*) (Table 1). To construct Cry1Aa mutants, the *Bt cry1Aa1* gene from pOS4101 (*5*), which originally came from pES1 (*22*), was subcloned into the pBluescript KS^- plasmid, to generate pBN-1Aa. To accommodate the *Nde*I fragment containing the *cry1Aa* coding region, the *Eco*RV recognition sequence in the multiple cloning site of the vector was modified to an *Nde*I recognition sequence by site-directed mutagenesis. The Cry1Aa mutant proteins were constructed using single-stranded DNA of the wild-type Cry1Aa as a template. Mutagenic oligonucleotide DNA primers were from GeneMed Synthesis, Inc. (South San Francisco, CA). Site-directed mutagenesis was performed according to the instructions of the manufacturer (Bio-Rad), with the single-stranded DNA template prepared using the Bio-Rad mutagenesis kit.

Bacterial cultures were grown overnight and screened by plasmid extraction followed by double-stranded DNA sequencing. Sequencing was performed in the PTC-150 Minicycler (MJ Research, Inc., MA) using the Perkin-Elmer

Applied Biosystems DNA sequencing kit following the instructions of the manufacturer. The sequencing results were analyzed using the ABI 373A DNA sequencer. Stock cultures were established from cultures grown overnight in 5 mL of LB liquid medium with 100 μg/mL ampicillin.

Toxin Preparation. A single colony obtained from LB/ampicillin agar plates of *Escherichia coli* MV1190 containing the mutant *cry1Aa1* gene was grown in 500 mL of terrific broth (TB) medium (*23*) (containing 100 μg/mL ampicillin) for 72 h at 37 °C, while shaking at 250 rpm. Cultures were centrifuged for 10 min at 8000 rpm. Pelleted cells were resuspended in lysis buffer [50 mM Tris at pH 8.0, 50 mM ethylenediaminetetraacetic acid (EDTA), 15% sucrose, and 10 μg/mL lysozyme] and then incubated for 2 h with shaking at 37 °C. Purification of inclusion bodies was performed as described (*17*). The final pellet was solubilized in 50 mM sodium carbonate buffer at pH 10.5 for 4 h, while shaking at 37 °C. Digestion of the protoxin was carried out by the addition of trypsin in a trypsin/protoxin ratio of 1:20 (wt/wt) for 1 h at 37 °C. An equivalent amount of trypsin was added, and the digestion procedure was repeated. Both protoxin and toxin were analyzed by 10% sodium dodecyl sulfate−polyacrylamide gel electrophoresis (SDS−PAGE).

Toxicity Bioassays. High-performance liquid chromatography (HPLC)-purified, trypsin-activated toxins were diluted in 50 mM carbonate buffer at pH 9.5. *Manduca sexta* bioassays were performed using the surface contamination method of intoxication. Each concentration of toxin was applied with a volume of 50 μL to a 2 cm^2 well containing artificial diet in a 24-well tissue culture plate (Falcon). Two neonate (2−4 days old) larvae were placed on each well, and analysis of insect mortality was recorded after 5 days. At least five concentrations for each toxin were used, and the lethal concentration at which 50% insect mortality (LC_{50}) occurred was obtained. *Bombyx mori* bioassays were carried out using the force-feeding method of intoxication. A single concentration of toxin was fed to fourth instar larvae in varying dosages. The larvae were then isolated and fed, and insect mortality was recorded after 24 h. At least five different dosages were used, and the lethal dosage at which 50% insect mortality (LD_{50}) occurred was obtained. The LC_{50} and LD_{50} were determined with the PROBIT method included in the computer program SoftTox (WindowChem Software, Inc.).

Secondary-Structure Analysis. Toxin was purified by size-exclusion chromatography with an Äkta Explorer workstation (Pharmacia, Sweden) with a HiLoad 16/60 Superdex200 column (Pharmacia). A 2 mL volume of toxin was eluted with 1 mM KH_2PO_4/K_2HPO_4 buffer at pH 7.4, previously filtered through 20 μm filter paper (Millipore). Conformational changes in the secondary structure were determined using circular dichroism (CD) spectroscopy. The spectra were collected with an AVIV CD2 spectropolarimeter at 25 °C in a 1 cm path-length quartz cuvette (Hellma). Each sample contained 30 μg of purified toxin diluted up to 3 mL with Milli-Q water. Ellipticity was measured as a function of the wavelength from 250 to 200 nm in 1 nm increments. Each CD spectra is the average of 10 scans. These data were used to calculate the contents of secondary structure (α helix, β sheet, and random coils) with the computer program K2D (*24*).

Thermal Denaturation Analysis. Toxin purification was performed as described under secondary-structure analysis. The stability of each toxin was determined by measuring the percentage of native protein as a function of temperature. CD spectral analysis was obtained at the single wavelength of 223 nm from 30 to 90 °C. Each sample contained 30 μg of toxin diluted up to 3 mL with Milli-Q water/1.5 M guanidine hydrochloride. Data were normalized by regression analysis to sigmoidal equations using SigmaPlot-2000 (Jandel Scientific Co.).

Binding Experiments. Brush border membrane vesicles (BBMV) were prepared from fifth instar *M. sexta* midguts by the magnesium precipitation method (*25*). Vesicles were resuspended in binding buffer (8 mM $NaHPO_4$/2 mM KH_2PO_4/150 mM NaCl at pH 7.4) to a final protein concentration of 1 mg/mL and stored in liquid nitrogen until further use. Iodination of toxins for competition and dissociation assays was carried out as described (*14*). The homologous competition assay was performed by competing 1 nM ^{125}I-labeled toxin with an increasing concentration of the same unlabeled toxin as described (*26*). For the dissociation experiments, 50 μg of *M. sexta* BBMV was incubated with 2 nM of either ^{125}I-labeled Cry1Aa or ^{125}I-labeled mutant proteins in 100 μL of binding buffer at room temperature. After 1.0 h of incubation, 500-fold excess of unlabeled toxin was added to the ^{125}I-labeled toxin−BBMV suspension. The reaction was stopped at various time intervals (0−60 min) by spinning down the mixture. The pellets were washed twice with 300 μL of binding buffer to remove any unbound toxin. The iodine content of the final pellets was determined in a gamma counter (Beckman instruments). Nonspecific binding was determined by adding together labeled toxin and 500-fold excess of the corresponding unlabeled toxin to the BBMV. Nonspecific binding was subtracted in the final data analysis. Binding data were analyzed with Sigma Plot (Jandel Scientific Co.).

Electrophysiology. Ion-channel formation was analyzed by voltage clamping using the technique established by Harvey et al. (*27*). Experimental conditions and procedures were as described (*17*). Each experiment was carried out in the presence and absence of 500 mM β-ME (Sigma). For each experiment, a fourth instar larva was chilled in ice for 15 min. Then, the peritrophic membrane and the gut contents were removed, and the isolated membrane was attached to a holder with an effective area of 0.1 cm^2. The holder was placed into the voltage-clamp chamber that was previously filled with buffer (*17*) under continuous oxygen. When the signal was stable for about 20 min, the voltage was clamped to 0 V. After the current was stable for 10 min, 10 μg of toxin was applied into the lumen side and the inhibition of the short-circuit current (I_{sc}) was recorded. The inhibition of I_{sc} was measured with a DVC-1000 voltage/current clamp (World Precision Instruments, Sarasota, FL) connected to a MacLab-4 (AD Instruments, Mountain View, CA). Data analysis was performed with SigmaPlot 2000 (Jandel Scientific Co.). Recorded data was normalized to the percentage of I_{sc} remaining. Each experiment was repeated at least 3 times. After toxin application, the time required for the I_{sc} to drop 10% from its initial value was defined as the lag time, T_0 (*17*, *28*). The rate of ion transport was determined by the normalized slope of the linear portion of the I_{sc} inhibition curve (in μA/min) as described by Liebig et al. (*28*).

Table 2: Toxicity Bioassays[a]

	B. mori LD_{50} (ng/cm^2)		*M. sexta* LC_{50} (ng/cm^2)	
protein	(−) β-ME	(+) β-ME	(−) β-ME	(+) β-ME
Cry1Aa	10.45 (7.10−14.10)	no change	3.23 (2.43−4.29)	no change
SS1	>4000	>4000	>4000	>4000
SS2	45.65 (25.92−61.24)	66.32 (32.08−98.53)	13.57 (7.00−28.03)	10.34 (5.42−21.11)
SS3	93.36 (44.39−169.69)	62.24 (35.58−291.45)	45.37 (24.87−110.80)	24.62 (8.30−55.96)
SS4	43.28 (31.94−56.26)	25.34 (18.48−42.57)	33.23 (16.31−215.22)	12.41 (2.34−23.88)
R99C			>4000	
A144C			37.31 (22.64−143.40)	

[a] The bioassays were performed using *B. mori* and *M. sexta* with or without β-ME. *B. mori* insects were force-feed, and *M. sexta* insects were intoxicated by the food-contamination method. Confidence limits at the 95% confidence level appear in parentheses. Control bioassays with β-ME in 50 mM carbonate buffer at pH 9.5 (no toxin) showed no toxicity.

RESULTS

Production of Stable Toxins. The techniques described previously were successful in the production of 130-kDa protoxins with the desired mutations as determined by DNA sequencing. The mutant protoxins were subsequently subjected to trypsin digestion. Each of the four mutant protoxins produced a stable trypsin-activated 66 kDa protein. The size and presence of each toxin and corresponding protoxin were determined by 10% SDS−PAGE (data not shown). As described below, the SS1 double-cysteine mutant showed the most dramatic changes in biological activity; thus, two single-cysteine mutant proteins were created, Arg99Cys (R99C) and Ala144Cys (A144C), that correspond to the individual mutations introduced to create the SS1 mutant protein. These two mutations also produced protoxins with the same size as the wild-type protein. The corresponding trypsin-activated toxins displayed the same size and stability as the Cry1Aa wild type.

Toxicity Bioassays. The biological activity of the mutant proteins was assessed using toxicity bioassays (Table 2). Two species of insect larvae were used for the bioassays: the silkworm and the tobacco hornworm. *B. mori* (silkworm) larvae were intoxicated by the force-feeding method to obtain the LD_{50}. Against *B. mori* mutant toxins, SS2 ($LD_{50} \approx 45.65$ ng/cm^2), SS3 ($LD_{50} \approx 93.36$ ng/cm^2), and SS4 ($LD_{50} \approx 43.28$ ng/cm^2) have decreased their toxicity 4-, 9-, and 4-fold, respectively, compared to the wild-type toxin ($LD_{50} \approx 10.45$ ng/cm^2). The biological activity of the SS1 mutant protein was particularly affected by the mutations because the toxicity was completely lost ($LD_{50} > 4000$ ng/cm^2, where 4000 ng/cm^2 was the maximum amount of toxin tested). Bioassays were repeated in the presence of 20 mM β-ME (Table 2). It was expected that some of the disulfide bridges would be broken; therefore, some toxicity would be recovered. The overlapping confidence limits indicate that there were no changes in toxicity levels in the presence of β-ME. The toxicity of the SS1 mutant remained unchanged, because there was no detectable recovery in toxicity levels up to the maximum concentration tested.

M. sexta (tobacco hornworm) larvae were intoxicated by the food-contamination method to obtain the LC_{50}. The toxicity effects are very similar in this insect as in the silkworm. Mutant toxins SS2 ($LC_{50} \approx 13.57$ ng/cm^2), SS3 ($LC_{50} \approx 45.37$ ng/cm^2), and SS4 ($LC_{50} \approx 33.23$ ng/cm^2) have decreased their toxicity with respect to the Cry1Aa wild-type toxin ($LC_{50} \approx 3.23$ ng/cm^2) 4-, 14-, and 10-fold, respectively. The biological activity of the SS1 mutant protein was again drastically affected by the mutations because the toxicity was completely lost ($LC_{50} > 4000$ ng/cm^2, maximum amount of toxin tested). Bioassays were performed in the presence of 20 mM β-ME (Table 2). The confidence limits indicate that significant differences are not detected. The SS1 mutant protein did not show any increase in toxicity levels. Toxicity assays on *M. sexta* with the single-cysteine mutant proteins making up the SS1 mutant protein revealed that the first site, R99C, completely eliminates the toxicity of the protein. The second site, A144C, showed an 11-fold decrease in toxicity compared to the Cry1Aa wild type (Table 2).

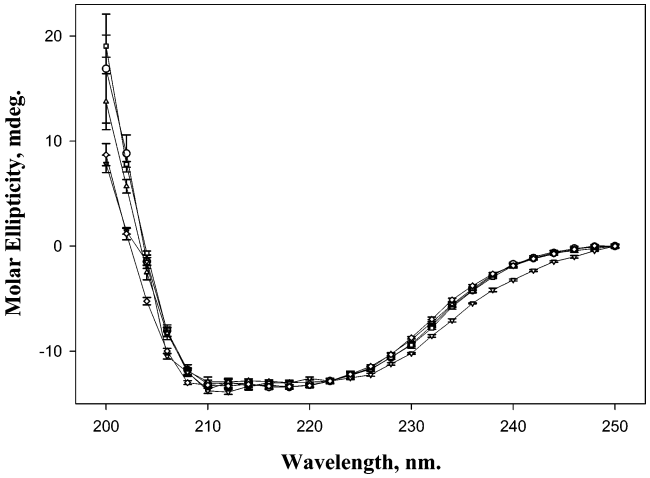

FIGURE 2: Structural analysis by CD. CD spectra for each toxin were collected at room temperature between 190−260 nm as the average of 10 scans. The secondary-structural contents for each protein were calculated with K2D (*24*) using data between 200 and 250 nm, as shown in the figure. The symbols used are (○) for Cry1Aa, (□) for SS1, (△) for SS2, (▽) for SS3, and (◇) for SS4. Slight conformational changes at the secondary-structural level are observed for mutant toxins SS3 and SS4 compared to the wild-type toxin.

Secondary-Structure Analysis. Conformational changes in the secondary structure of the mutant proteins, relative to the wild-type protein, determined by CD spectroscopy are shown in Figure 2. The ratios of the n−π* transition, that is responsive to the α-helical content at $\lambda = 223$ nm, $[\theta]_{223}$, and the $\pi-\pi$* excitation band at $\lambda = 208$ nm, $[\theta]_{208}$, for each protein are shown in the first column of Table 3. Two mutant proteins, SS1 ($[\theta]_{223}/[\theta]_{208} = 1.10$) and SS2 ($[\theta]_{223}/[\theta]_{208} = 1.09$) are virtually identical to the wild-type Cry1Aa ($[\theta]_{223}/[\theta]_{208} = 1.11$). The other two mutant proteins SS3 ($[\theta]_{223}/[\theta]_{208} = 1.05$) and SS4 ($[\theta]_{223}/[\theta]_{208} = 1.02$) display a decrease in the ellipticity ratio. The calculation of secondary-structural contents with K2D (*24*) (Table 3) indicates that SS1 is virtually identical to the wild-type toxin, with a spectrum that almost overlaps with the spectrum of the wild-type toxin (Figure 2). The α-helical contents of SS2, SS3, and SS4 increased by 23.3, 30.0, and 73.3%, respectively, compared to the α-helical contents of the wild-type toxin. In contrast, the β-sheet contents of SS2, SS3, and SS4 decreased by 31.8, 68.20, and 27.3%, respectively (Table

Table 3: Structural Analysis by CD[a]

protein	$[\theta]_{223}/[\theta]_{208}$	percent α helix[b]	percent β sheet[b]	percent other[b]	T_m[c] (°C) (−) β-ME	T_m[c] (°C) (+) β-ME
Cry1Aa[d]		33.1[d]	19.75[d]	47.15[d]		
Cry1Aa	1.11	30 ± 2.82	22 ± 2.25	48 ± 0.85	69.46 ± 0.98	69.55 ± 1.30
SS1	1.10	35 ± 3.29	19 ± 1.94	46 ± 0.08	69.46 ± 1.09	70.43 ± 1.45
SS2	1.09	37 ± 3.47	15 ± 1.53	48 ± 0.84	70.72 ± 1.45	68.91 ± 0.90
SS3	1.05	39 ± 3.66	7 ± 0.71	54 ± 0.95	68.73 ± 1.16	66.19 ± 1.09
SS4	1.02	52 ± 4.88	16 ± 1.63	33 ± 0.58	68.73 ± 1.34	66.73 ± 0.98

[a] The secondary-structure contents of each toxin were calculated with K2D using CD data. The crystallographic data and the values calculated from CD spectra for the Cry1Aa wild-type toxin are virtually identical. The thermal denaturation analysis was used to calculate the stability of the mutant proteins compared to the Cry1Aa wild type (columns 6 and 7). [b] Obtained with K2D from the CD spectra shown in Figure 2. [c] T_m, temperature at which 50% of the protein population reaches the unfolded state. [d] Obtained from the crystallographic data (PDB code 1CIY).

3). The remaining secondary structure is classified as random coils and other structures. It is decreased by 4.2% in SS1, unchanged in SS2, increased by 12.5% in SS3, and decreased by 31.2% in SS4, compared to the wild type. To assess the accuracy of the K2D calculations, results obtained for the wild-type protein were compared to the secondary-structural contents obtained by X-ray diffraction (PDB code 1CIY). These results are very close to the conformations predicted by CD, as shown in the first row of Table 3. Although there were slight structural changes in the secondary structure of the SS2, SS3, and SS4 mutant proteins, none of them was drastic enough to alter the resistance to protease digestion.

Thermal Denaturation Analysis. Protein stability was also determined by thermal unfolding analysis monitored by CD (Figure 3 and columns 6 and 7 in Table 3). It has been observed that thermal unfolding of Cry toxins is an irreversible process (Alzate and Dean, unpublished observation; *29*); however, thermal unfolding can be used to determine the temperature at which approximately 50% of the protein population reaches the unfolded state (T_m). This temperature was found for each mutant protein by following the CD spectrum of the α-helical signal at $\lambda = 223$ nm as a function of temperature. When no reducing agent was present (Figure 3A and column 6 in Table 3), essentially all mutant proteins have the same melting temperature as the wild-type protein ($T_m = 69.46 \pm 0.98$ °C). However, the unfolding behavior displayed on temperatures above T_m indicates that SS3 and SS4 reach the unfolded state at almost the same rate as the wild-type protein, while mutant proteins SS1 and SS2 need about 4.0 °C more than the wild type to reach the unfolded state (Figure 3A). A partial unfolded state seems to have been slightly stabilized in SS1 and SS2 that could result from disulfide bridge formation.

The unfolding process in the presence of 20 mM β-ME (Figure 3B and column 7 in Table 3) indicates that SS1 and SS2 have a similar melting temperature as the wild-type toxin ($T_m = 69.55 \pm 1.30$ °C). Mutant toxins SS3 and SS4 have decreased their melting temperatures by about 3.0 °C with respect to the wild type. In addition, SS3 and SS4 start unfolding at lower temperatures (~62 °C for SS3 and ~53 °C for SS4) than the wild type toxin, suggesting that SS3 and SS4 are less stable in the reduced state (Figure 3B).

Binding Experiments. Homologous competition binding experiments were performed to determine the binding affinity of the wild-type and mutant toxins on *B. mori* and *M. sexta* BBMV. Analysis of competition binding experiments indicates that the mutant proteins, both the toxic SS2, SS3, and SS4 and the nontoxic SS1, do not display significant differences in K_d as compared to the wild-type Cry1Aa toxin ($K_d = 0.2798 \pm 0.037$ nM). We tested the ability of the toxins to remain membrane-bound by dissociation of proteins preincubated with BBMV. Our results indicate that on either *B. mori* or *M. sexta* BBMV, the proteins have the same binding parameters as the wild-type toxin (data not shown).

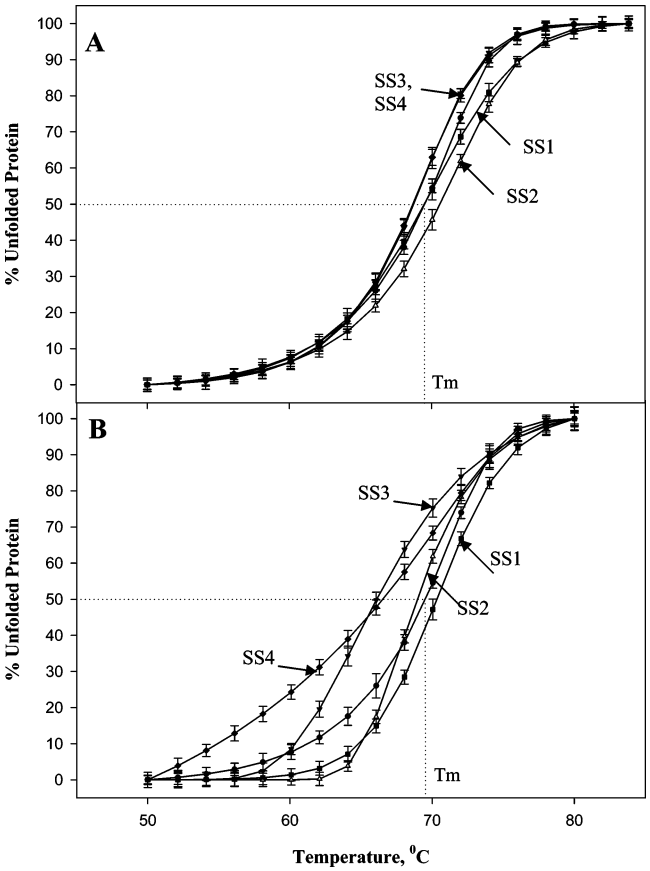

FIGURE 3: Thermal unfolding of wild-type and mutant proteins. (A) Protein unfolding in the absence of β-ME. (B) Protein thermal unfolding in the presence of β-ME. Symbols are the same as in Figure 2: (○) Cry1Aa, (□) SS1, (△) SS2, (▽) SS3, and (◇) SS4. Dashed lines indicate T_m, the temperature at which approximately 50% of the protein population is in the unfolded state.

Electrophysiology. The toxin-induced decrease in the short circuit current, I_{sc}, of voltage-clamped midgut membranes has been used as a measure of the toxic activity of Cry proteins, for which a close correlation between ion-channel formation and toxic action has been shown (*14*). The ion-channel activity induced by the Cry1Aa and SS mutant proteins in *M. sexta* midgut membranes in the absence and presence of the reducing agent is displayed in parts A and

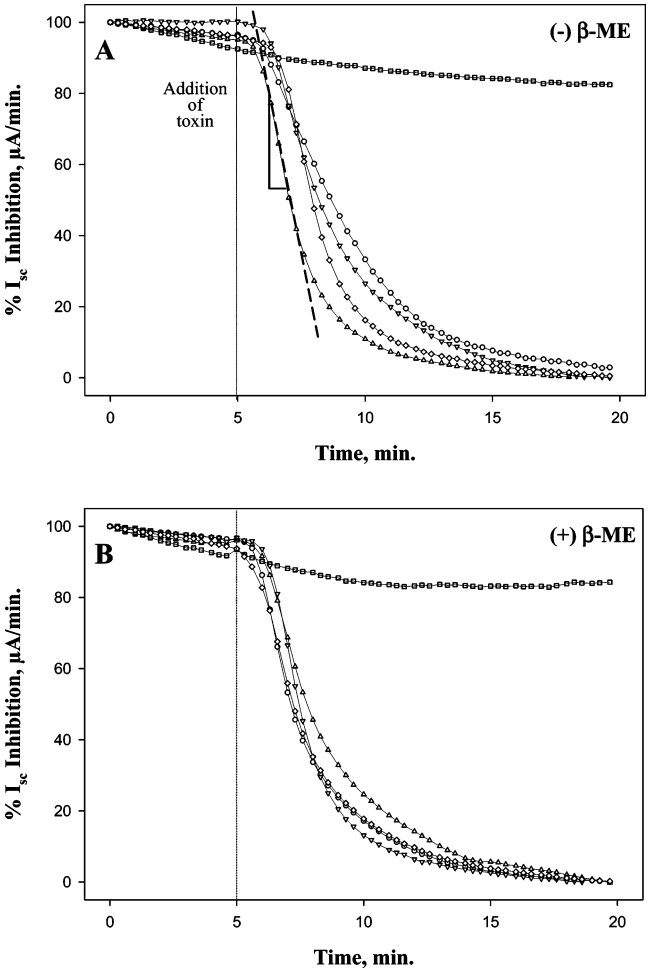

FIGURE 4: Voltage-clamping analysis on insect midgut membranes. (A) Ion-channel formation in the absence of the reducing agent. All proteins but SS1 display ion-channel formation. (B) Ion-transport activity in the presence of β-ME. The symbols used are (○) for Cry1Aa, (□) for SS1, (△) for SS2, (▽) for SS3, and (◇) for SS4. The short-dashed line indicates the time at which the toxin was added to the voltage-clamp chambers, and the long-dashed line and triangle show how the slope was calculated.

Table 4: Voltage-Clamping Parameters Determined on *M. sexta* Midgut Membranes[a]

	T_0[b] (min)		slope[c] (μA/min)	
protein	(−) β-ME	(+) β-ME	(−) β-ME	(+) β-ME
Cry1Aa	0.90 ± 0.11	0.78 ± 0.09	−15.93 ± 1.33	−23.09 ± 2.19
SS1[d]				
SS2	0.70 ± 0.08	1.10 ± 0.13	−28.78 ± 2.73	−18.05 ± 1.71
SS3	0.72 ± 0.09	1.24 ± 0.15	−17.66 ± 1.67	−28.63 ± 2.71
SS4	1.50 ± 0.18	0.38 ± 0.04	−29.83 ± 2.83	−23.27 ± 2.21

[a] Parameters shown are calculated from data displayed in Figure 4. [b,c] T_0 and slope were calculated as described in Liebig et al. (*28*). The slope of the falling I_{sc} is indicated by the triangle and the sloping line shown in Figure 4A. The lag time, T_0, is taken as the time needed for the I_{sc} current to drop 10% from its value in the absence of toxin (*17*, *28*). [d] The SS1 mutant protein did not show I_{sc}.

B of Figure 4, respectively. Table 4 shows the data calculated from Figure 4. The lag time, taken as an indication of the rate of protein partitioning into BBMV, indicates that the ability of Cry1Aa to penetrate the membrane is the same with or without β-ME (T_0 with β-ME overlaps T_0 without β-ME; Figure 4B and Table 4). No lag time is detected for the SS1 mutant protein. As shown in Table 2 and Figure 4, the SS1 mutant protein did not display toxicity *in vivo* (bioassays) or *in vitro* (T_0 and slope). The other three mutant proteins conserve their ability to penetrate into the membrane. In the absence of β-ME, only SS4 is significantly slower than the wild type to penetrate the membrane, as indicated by a lag time of 1.5 min, compared to 0.9 min for the wild-type toxin. In the presence of β-ME, SS4 displays a detectable reduction in the lag time ($\Delta T_0 = -1.12$ min) compared to its T_0 in the absence of β-ME. SS2 ($\Delta T_0 = +0.40$ min) and SS3 ($\Delta T_0 = +0.52$ min) showed slight delays in membrane partitioning with the reducing agent. What is critical from these lag-time observations is the capacity of the mutant toxins to form ion channels, both in the oxidized and in the reduced states, indicating the ability of the toxin to form ion channels in a conformation in which the α helices of domain I do not need to separate from each other.

The slope obtained from voltage clamping is a measure of the ion-transport activity. The addition of the reducing agent has different effects on the ion-channel activity of the proteins. In the first place, it is observed that the ion-channel activity of Cry1Aa changes from −15.95 μA/min in the absence of β-ME to −23.09 μA/min in the presence of β-ME, an increase of 45% (Table 4). Such an effect, which will not be explored here, suggests that there are unknown interactions between the reducing agent and membrane components. This effect that is not observed on the lag time indicates that the partitioning into the membrane is not affected by the β-ME. Second, there is no ion-channel activity by the SS1 mutant protein, suggesting that either the disulfide bridge was not formed or was not accessible to the reducing agent or the mutations by themselves were drastic enough to eliminate the biological activity of the mutant. This last possibility was explored by creating the R99C and A144C single-mutant proteins. As shown in Table 2, the biological activity of the R99C mutant protein is eliminated and the activity by A144C is reduced 11.5-fold, explaining why the reduction of the disulfide bridge did not recover ion-channel formation by the SS1 mutant protein.

The ion-channel activity by the SS2 mutant protein is decreased by about 37% in the presence of β-ME, showing that these two residues have large effects in the ion channel, because the β-ME by itself increases this activity by 45%. Contrary to SS2, SS3 displayed an increase in ion-channel formation by about 62%, larger than the increase induced by β-ME (45%). The SS4 mutant protein, which displays a longer time for membrane partitioning (Table 4), shows a decrease of ∼22% in ion-channel activity.

DISCUSSION

The *Bt* protein toxins have the ability to incorporate into specific biological membranes of target insects. The insertion mechanism and the topological organization of the protein in the membrane-bound state are currently unknown. It was proposed that the *Bt* δ-endotoxins organize into the membrane following a mechanism proposed earlier for colicin A1. Since then, it has been believed that the *Bt* toxins follow such organization steps. In an attempt to address these issues, Schwartz et al. (*4*) introduced double-cysteine mutations in the *cry1Aa* gene and performed physiological studies on artificial phospholipid membranes.

Following similar approaches, we introduced the same double-cysteine mutations described by Schwartz et al. into the Cry1Aa toxin to form disulfide bridges (Figure 1 and Table 1). The formation of such bridges would hold some conformations but not permit the partition of the toxin into the membrane as proposed by the umbrella model. The effects of these mutations on the toxicity of the resulting proteins, on their ability to form ion channels, and on the structure of these proteins were assessed as a mechanistic approach to test the validity of the models in biological membranes of susceptible insects.

Toxicity assays reveal that the SS1 mutant protein (R99C−A144C) did not show any toxic effect up to the maximum concentration tested (4000 ng/cm^2). The other three mutant toxins have reduced toxicity compared to the wild-type toxin. Against *M. sexta*, SS2, SS3, and SS4 are 4, 14, and 10 times less toxic than the wild-type protein, respectively. Some reasons could be argued to explain the drop in toxicity of the mutant proteins, including (i) structural alterations resulting from the mutations, (ii) the formation of the disulfide bridges, (iii) the direct involvement of the mutated residues in the protein−receptor binding interaction, and (iv) the direct involvement of the altered residues in ion-channel activity.

The possibility of the toxicity loss as a result of conformational changes was examined by analyzing the secondary structure of the proteins via CD (Figure 2 and Table 3). From the information contained in the Protein Data Bank, it is known that the Cry1Aa toxin has 33.10% α-helix, 19.75% β-sheet, and 47.15% remaining secondary structure and random-coil conformations. Our calculated secondary-structural contents for the wild-type protein derived from CD using K2D indicate that the contents of α helix is 30 ± 2.82%, of β sheet is 22 ± 2.25%, and of other secondary-structural contents is 48 ± 0.85%, in agreement with the crystallographic data. On the basis of these results, it is clear that there are no CD-detectable changes in the structure of the SS1 mutant protein. On the other hand, SS2, SS3, and SS4 have increased their α-helical contents while decreasing their amount of β-sheet conformations. These results suggest that in SS2, SS3, and SS4 the disulfide bridges were formed, because more rigid α-helical conformations will lead to a higher α-helical CD signal. SS4 shows the highest increase in α-helical contents, suggesting that a larger portion of domain I has reduced mobility, as expected from domain I being strongly linked to domain II. This is further supported by the small change in the amount of β sheet and the considerable decrease in the random-coil conformation displayed by SS4. SS3 has a considerable increase in random coil, suggesting a tendency toward more unfolded domains II and/or III. The packing of domain I was also affected in mutant toxins SS3 and SS4 as evidenced by the $[\theta]_{223}/[\theta]_{208}$ ratio (Table 3). Nonetheless, none of the mutations altered the proteins to a level that would make them susceptible to protease digestion as determined by 10% SDS−PAGE. It is reasonable to conclude, on the basis of the CD data, that the lack of toxicity in SS1 is not the result of changes in the secondary structure of the protein and that disulfide bridges were formed in SS2, SS3, and SS4.

We then tested whether the disulfide bridges had effects on insecticidal activity. Toxic levels were determined in the presence of β-ME to reduce the disulfide bridges. The proteins were either mixed with 200 times molar excess of β-ME or preincubated over a 12 h period previous to the test. There were no significant changes in toxicity levels compared to the results without β-ME (Table 2). These results could be explained by several possibilities. It could be that the disulfide bridges were reduced in the insect midgut; therefore, bioassays in the absence and presence of β-ME will not make any difference. Another possibility would be a protein inserting in the midgut membrane as a whole molecule or at least domains I and II together; therefore, the presence of disulfide bridges limiting the separations of the α helices in domain I will not have significant contributions to toxicity levels. It also could be that the disulfide bridges are not affected by the reducing agent and that the midgut environment is not strong enough to reduce those disulfide bridges.

We tested whether the disulfide bridges were reduced by β-ME using thermal denaturation analysis followed by CD. On the basis of our experience with disulfide introduction into Cry3Aa (*30*), we expected the melting curve of the SS mutants in Cry1Aa to show an increase in the T_m temperature. As shown in Figure 3A, in the absence of β-ME, changes in T_m were small and not easily attributable to disulfide bridge formation. However, in the presence of β-ME, SS2, SS3, and SS4 have decreased their T_m, suggesting that the disulfide bridges were broken by the reducing agent (Figure 3B). The decrease in T_m is particularly large for SS3 and SS4, indicating that these mutant proteins were readily affected by the absence of the wild-type amino acid residues. SS3 shows a clear deviation from the wild-type stability by starting to unfold at about 62 °C, while the SS4 mutant protein starts unfolding at about 53 °C. These changes in structural stability explain the decrease in toxicity levels observed for SS3 and SS4 in the reduced state. It is also seen that a partially folded conformation is stabilized in SS1 and SS2 that likely results from the presence of a disulfide bridge, which is reduced by β-ME, allowing the proteins to recover their wild-type-like thermal stability. The data presented up to this point are sufficient to conclude that SS1, SS2, SS3, and SS4 have formed disulfide bridges, that these disulfide bridges are reduced by β-ME, and that the reduction of toxicity displayed by SS3 and SS4 is likely to result from structural alterations detected in the reduced state.

The possibility that the disulfide bridges are reduced by the insect midgut and, therefore, that the addition of β-ME will not have an effect on toxicity assays was further studied by analyzing the ion-transport activity of these mutant proteins in insect midgut membranes. As observed in Figure 4A, the SS2, SS3, and SS4 mutant proteins conserved their ion-channel function in the absence of the reducing agent. A detailed observation of the ion-transport parameters, T_0 and slope, shed some light to the membrane−protein interaction. The lag time for Cry1Aa in the absence and presence of β-ME is the same, indicating that the reducing agent has no effect on protein translocation into the midgut membrane. The lag times for the intrahelical disulfide bridges, SS2 and SS3, under reducing conditions are longer than the lag times under nonreducing conditions. These results suggest that a more rigid, more organized α-helical domain I has a better ability to translocate into the membranes. These results are in agreement with previous studies, proposing that some α helices were important for the

initiation of the protein translocation process (*13*). The lag time for SS4 shows that under nonreducing conditions this protein is slower inserting into the membrane, a property that is recovered by the reduction of the disulfide bridge. This demonstrates that the disulfide bridges are not reduced by the midgut alone and that a separation of domain I from domain II is important for the initiation of the translocation process. Analysis of the ion-transport activities, the slope, is a little more complicated because individual amino acid substitutions have an effect on toxicity and the presence of β-ME has a substantial effect on this process as shown by changes in the slope for Cry1Aa under reducing and nonreducing conditions. However, it is important to realize that, with the exception of SS1, the remaining mutant toxins have ion-transport ability, suggesting that the disulfide bridges did not impede protein translocation into the membrane.

A particular situation is observed with the SS1 mutant protein. There was not detectable toxicity against any of the insects, under either oxidizing or reducing conditions. Structural changes were not observed, and ion-transport activity was undetected for this mutant protein. Before concluding that α helices 3 and 4 need to be free from each other for the protein to form ion channels, we tested the effects of the individual mutations. Both residues, Arg99 and Ala144, have affected the toxicity levels of the protein (Table 2). The fact that Arg99Cys eliminated the toxic effect of the protein suggests that Arg at position 99 is required for toxicity. The lack of toxicity was the result of removing the arginine residue from such a position and not the result of the disulfide bridge formation; therefore, this mutant protein does not offer functional information concerning the insertion mechanism of Cry1A toxins in biological membranes.

The main goal for this research was to obtain information about the insertion process of Cry1Aa into the midgut membrane of two lepidopteran insects. The double-cysteine mutations in the SS1, SS2, SS3, and SS4 Cry1Aa mutant proteins were introduced to form disulfide bridges. It is observed that SS2, SS3, and SS4 have reduced their toxicity levels, but it has not been eliminated completely. The SS1 mutant toxin, designed to form a disulfide bridge between α helices 3 and 4, lost all toxic activity that was neither the result of conformational nor structural alterations. The locking of α helices 5 and 6 by SS2, α helices 5 and 7 by SS3, or domain I and domain II by SS4 was a factor that neither prevented the toxins to partition into the membrane nor eliminated ion-transport activity. However, eliminating the disulfide bridge in SS4 reduced the partition time, suggesting that some degree of freedom helps the penetration of the toxin into the membrane.

We and others have demonstrated that α helix 7 of Cry1A also participates in ion transport (*14*, *15*). We demonstrated that the preincubation of Cry1Ab with BBMV protects the whole toxin from proteolytic digestion by proteinase K (*17*). In a more recent work, Tomimoto et al. (*20*) have proposed a "buried dragon model" in which the whole protein associates with the midgut membrane and is protected from digestion by pronase. The data presented here indicate that there is no need for the α helices to separate from each other for the protein to partition in the midgut membrane and therefore to be toxic. These results do not support protein partition models in which individual α-helical hairpins are required to penetrate the membrane by themselves. Rather, an alternative model, in which the protein partitions as a whole molecule in the lipid environment, will be in better agreement with these data.

REFERENCES

1. Schnepf, E., Crickmore, N., van Rie, J., Lereclus, D., Baum, J., Feitelson, J., Zeigler, D. R., and Dean, D. H. (1998) *Bacillus thuringiensis* and its pesticidal crystal proteins, *Microbiol. Mol. Biol. Rev. 62*, 775−806.
2. Grochulski, P., Masson, L., Borisova, S., Pusztai-Carey, M., Schwartz, J. L., Brousseau, R., and Cygler, M. (1995) *Bacillus thuringiensis* CryIA(a) insecticidal toxin: Crystal structure and channel formation, *J. Mol. Biol. 254*, 447−464.
3. Li, J. D., Carroll, J., and Ellar, D. J. (1991) Crystal structure of insecticidal δ-endotoxin from *Bacillus thuringiensis* at 2.5 Å resolution, *Nature 353*, 815−821.
4. Schwartz, J. L., Juteau, M., Grochulski, P., Cygler, M., Prefontaine, G., Brousseau, R., and Masson, L. (1997) Restriction of intramolecular movements within the Cry1Aa toxin molecule of *Bacillus thuringiensis* through disulfide bond engineering, *FEBS Lett. 410*, 397−402.
5. Ge, A. Z., Shivarova, N. I., and Dean, D. H. (1989) Location of the *Bombyx mori* specificity domain on a *Bacillus thuringiensis* δ-endotoxin protein, *Proc. Natl. Acad. Sci. U.S.A. 86*, 4037−4041.
6. Lu, H., Rajamohan, F., and Dean, D. H. (1994) Identification of amino acid residues of *Bacillus thuringiensis* δ-endotoxin CryIAa associated with membrane binding and toxicity to *Bombyx mori*, *J. Bacteriol. 176*, 5554−5559.
7. Rajamohan, F., Hussain, S. R., Cotrill, J. A., Gould, F., and Dean, D. H. (1996) Mutations at domain II, loop 3, of *Bacillus thuringiensis* CryIAa and CryIAb δ-endotoxins suggest loop 3 is involved in initial binding to lepidopteran midguts, *J. Biol. Chem. 271*, 25220−25226.
8. Lee, M. K., Young, B. A., and Dean, D. H. (1995) Domain III exchanges of *Bacillus thuringiensis* CryIA toxins affect binding to different gypsy moth midgut receptors, *Biochem. Biophys. Res. Commun. 216*, 306−312.
9. de Maagd, R. A., Kwa, M. S., van der Klei, H., Yamamoto, T., Schipper, B., Vlak, J. M., Stiekema, W. J., and Bosch, D. (1996) Domain III substitution in *Bacillus thuringiensis* δ-endotoxin CryIA(b) results in superior toxicity for *Spodoptera exigua* and altered membrane protein recognition, *Appl. Environ. Microbiol. 62*, 1537−1543.
10. Hodgman, T. C., and Ellar, D. J. (1990) Models for the structure and function of the *Bacillus thuringiensis* δ-endotoxins determined by compilational analysis, *DNA Sequence 1*, 97−106.
11. Lakey, J. H., Gonzalez-Manas, J. M., van der Goot, F. G., and Pattus, F. (1992) The membrane insertion of colicins, *FEBS Lett. 307*, 26−29.
12. Parker, M. W., Tucker, A. D., Tsernoglou, D., and Pattus, F. (1990) Insights into membrane insertion based on studies of colicins, *Trends Biochem. Sci. 15*, 126−129.
13. Gazit, E., La Rocca, P., Sansom, M. S., and Shai, Y. (1998) The structure and organization within the membrane of the helices composing the pore-forming domain of *Bacillus thuringiensis* δ-endotoxin are consistent with an "umbrella-like" structure of the pore, *Proc. Natl. Acad. Sci. U.S.A. 95*, 12289−12294.
14. Alcantara, E. P., Alzate, O., Lee, M. K., Curtiss, A., and Dean, D. H. (2001) Role of α-helix seven of *Bacillus thuringiensis* Cry1Ab δ-endotoxin in membrane insertion, structural stability, and ion channel activity, *Biochemistry 40*, 2540−2547.
15. Chandra, A., Ghosh, P., Mandaokar, A. D., Bera, A. K., Sharma, R. P., Das, S., and Kumar, P. A. (1999) Amino acid substitution in α-helix 7 of Cry1Ac δ-endotoxin of *Bacillus thuringiensis* leads to enhanced toxicity to *Helicoverpa armigera* Hubner, *FEBS Lett. 458*, 175−179.
16. Dean, D. H., Rajamohan, F., Lee, M. K., Wu, S. J., Chen, X. J., Alcantara, E., and Hussain, S. R. (1996) Probing the mechanism of action of *Bacillus thuringiensis* insecticidal proteins by site-directed mutagenesis−A minireview, *Gene 179*, 111−117.
17. Arnold, S., Curtiss, A., Dean, D. H., and Alzate, O. (2001) The role of a proline-induced broken-helix motif in α-helix 2 of *Bacillus thuringiensis* δ-endotoxins, *FEBS Lett. 490*, 70−74.
18. Aronson, A. I., and Shai, Y. (2001) Why *Bacillus thuringiensis* insecticidal toxins are so effective: Unique features of their mode of action, *FEMS Microbiol. Lett. 195*, 1−8.

19. Loseva, O. I., Tiktopulo, E. I., Vasiliev, V. D., Nikulin, A. D., Dobritsa, A. P., and Potekhin, S. A. (2001) Structure of Cry3A δ-endotoxin within phospholipid membranes, *Biochemistry 40*, 14143−14151.
20. Tomimoto, K., Hayakawa, T., and Hori, H. (2006) Pronase digestion of brush border membrane-bound Cry1Aa shows that almost the whole activated Cry1Aa molecule penetrates into the membrane, *Comp. Biochem. Physiol., B: Biochem. Mol. Biol. 144*, 413−422.
21. Bravo, A., Gomez, I., Conde, J., Munoz-Garay, C., Sanchez, J., Miranda, R., Zhuang, M., Gill, S. S., and Soberon, M. (2004) Oligomerization triggers binding of a *Bacillus thuringiensis* Cry1Ab pore-forming toxin to aminopeptidase N receptor leading to insertion into membrane microdomains, *Biochim. Biophys. Acta. 1667*, 38−46.
22. Schnepf, H. E., and Whiteley, H. R. (1981) Cloning and expression of the *Bacillus thuringiensis* crystal protein gene in *Escherichia coli*, *Proc. Natl. Acad. Sci. U.S.A. 78*, 2893−2897.
23. Sambrook, J., Fritsch, E. F., Maniatis, T. (1989) *Molecular Cloning: A Laboratory Manual*, 2 ed., Cold Spring Harbor Laboratory Press, Plainview, NY.
24. Andrade, M. A., Chacon, P., Merelo, J. J., and Moran, F. (1993) Evaluation of secondary structure of proteins from UV circular dichroism spectra using an unsupervised learning neural network, *Protein Eng. 6*, 383−390.
25. Wolfersberger, M. G. (1993) Preparation and partial characterization of amino acid transporting brush border membrane vesicles from the larval midgut of the gypsy moth (*Lymantria dispar*), *Arch. Insect Biochem. Physiol. 24*, 139−147.
26. Liang, Y., Patel, S. S., and Dean, D. H. (1995) Irreversible binding kinetics of *Bacillus thuringiensis* CryIA δ-endotoxins to gypsy moth brush border membrane vesicles is directly correlated to toxicity, *J. Biol. Chem. 270*, 24719−24724.
27. Harvey, W. R., Crawford, D. N., and Spaeth, D. D. (1990) Isolation, voltage clamping, and flux measurements in lepidopteran midgut, *Methods Enzymol. 192*, 599−608.
28. Liebig, B., Stetson, D. L., and Dean, D. H. (1995) Quantification of the effect of *Bacillus thuringiensis* toxins on short-circuit current in the midgut of *Bombyx mori*, *J. Insect Physiol. 41*, 17−22.
29. Potekhin, S. A., Loseva, O. I., Tiktopulo, E. I., and Dobritsa, A. P. (1999) Transition state of the rate-limiting step of heat denaturation of Cry3A δ-endotoxin, *Biochemistry 38*, 4121−4127.
30. Wu, S. J. (1996) in *Biochemistry*, The Ohio State University, Columbus, OH.

BI061474Z